Investigation of the dosage effect on the activation of arsenic- and boron-implanted low-pressure chemical vapor deposition (LPCVD) amorphous-silicon films

Fang-Shing Wang [a], Meng-Jin Tsai [b], Wen-Koi Lai [a], Huang-Chung Cheng [a,*]

[a] *Department of Electronics Engineering and Institute of Electronics, National Chiao Tung University, Hsinchu, Taiwan, ROC*
[b] *United Microelectronics Corp., Hsinchu, Taiwan, ROC*

Abstract

The dopant activation of arsenic- and boron-implanted low-pressure chemical vapor deposition (LPCVD) amorphous silicon (α-Si) films, furnace-annealed with different annealing temperatures has been investigated. For the arsenic-implanted specimens with a dosage of 4×10^{14} cm^{-2}, an increase of sheet resistance was observed with increasing annealing temperature for the temperatures range from 700 to 850°C. The reverse annealing phenomenon is attributed to dopant segregation at grain boundaries and becomes less marked with heavier doped films (2×10^{15} cm^{-2}). Consequently for a dosage of 1×10^{16} cm^{-2}, the sheet resistance exhibits a monotonic decrease with increasing annealing temperature. As for the boron-implanted specimens, the reverse annealing phenomenon is not observed. It means that dopant segregation is not significant for boron-implanted films.

1. Introduction

Polycrystalline silicon (poly-Si) deposited by the low-pressure chemical vapor deposition (LPCVD) technique is extensively used in modern very-large scale integrated (VLSI) devices [1]. The doped poly-Si films are generally used as the interconnection lines between devices, gate electrode materials for MOSFETs, load resistors for SRAMs, and poly-emitter contacts for bipolar devices, etc. [2]. For the latter two applications, the required doping can be accomplished with precise control by use of ion implantation [3]. The activation of the doped poly-Si or α-Si films has been achieved by using annealing

techniques such as furnace annealing [4], rapid thermal annealing [5], as well as laser annealing [6]. Both the As$^+$ and B$^+$ are generally used as the n-type and p-type dopants in Si processing. In this paper, the furnace annealing of As$^+$- and B$^+$-implanted α-Si films has been investigated. With the annealing temperature varying from 600 to 1100°C, the dosage effects of the specimens for the different annealing temperatures have been observed and discussed.

2. Experimental procedures

Three inch diameter, (100) oriented, n-type silicon wafers were used as the substrates. After a field
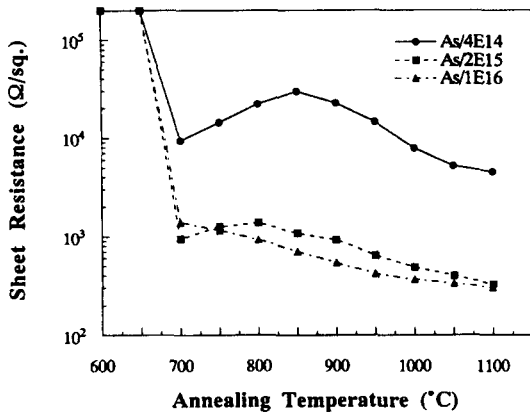
* Corresponding author. Fax: 886 35 724361.

Fig. 1. Sheet resistances of the As^+-implanted specimens annealed at different temperatures.
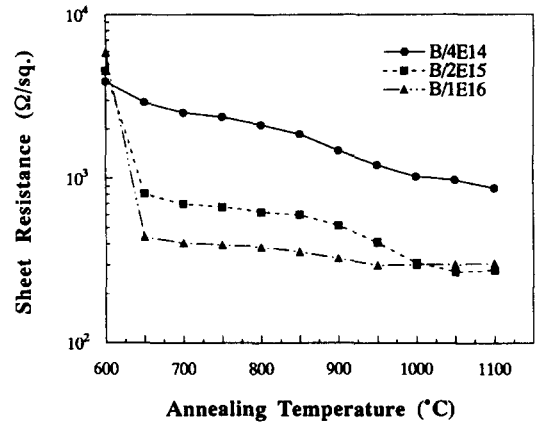

Fig. 2. Sheet resistance of the B^+-implanted specimens annealed at different temperatures.

oxide was thermally grown, an undoped α-Si film of thickness 100 nm was deposited by LPCVD at 550°C. The samples were As^+-implanted at an energy of 70 keV or B^+-implanted at an energy of 15 keV to the dosages of 4×10^{14}, 2×10^{15}, and 1×10^{16} cm^{-2}, respectively. After cleaning, the samples were capped with a layer of 200 nm PECVD oxide to prevent dopant outdiffusion in the subsequent annealing process. The specimens were furnace-annealed in N_2 ambient for 1 h in the temperature range from 600 to 1100°C to study dopant activation at different temperatures. The encapsulation oxide was then dipped in a dilute HF solution. The sheet resistance, effec-

tive carrier concentration, and electron mobility of the annealed poly-Si films were determined by the four-point probe and the Hall measurement apparatus. Transmission electron microscope (TEM) observations of these annealed specimens were performed to find the microstructure of poly-Si grains.

3. Results and discussion

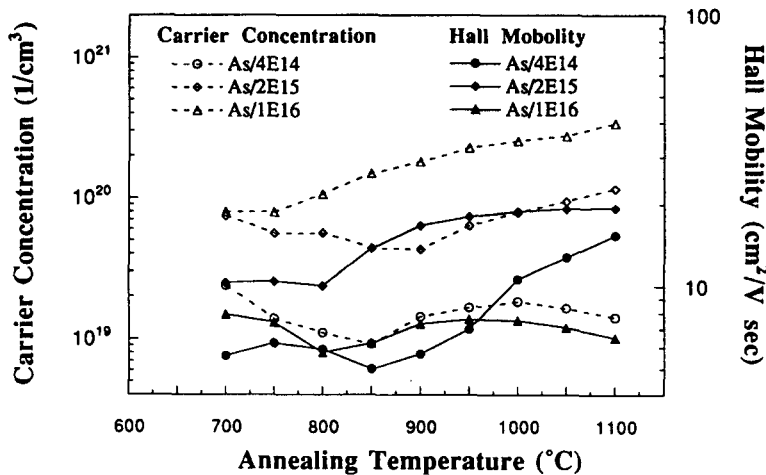Fig. 1 shows the curves of the sheet resistance versus the annealing temperature in the range from

Fig. 3. Carrier concentrations and mobilities of the As^+-implanted samples treated with different annealing temperatures.

600 to 1100°C for various As$^+$ implantation dosages. It is seen that for an annealing temperature below 700°C, the extremely high value of the sheet resistance implies inactivation of the implanted ions. The sheet resistances of the 1×10^{16} cm^{-2} samples show a monotonous decrease with increasing annealing temperatures above 700°C. For the specimens with the 2×10^{15} cm^{-2} dose, it is seen that between 700 and 800°C, the sheet resistance increases with increasing annealing temperature. This reverse annealing phenomenon becomes even more marked for the 4×10^{14} cm^{-2} implanted film, which has a maximum sheet resistance at the annealing temperature of 850°C. As for the B$^+$-implanted samples with the three kinds of dosages shown in Fig. 2, the sheet resistance monotonically decrease with increasing annealing temperatures. No reverse annealing phenomenon is found for the B$^+$-doped ones.

To further study the dopant activation of the implanted ions, the mobility and carrier concentration were also measured by the Hall measurement apparatus with the van der Pauw method. Figs. 3 and 4 show the carrier concentrations and mobilities corresponding to the results shown in Figs. 1 and 2, respectively. For the As$^+$-implanted samples, the carrier concentration of the 1×10^{16} cm^{-2} dose exhibits an increase with annealing temperature. However, the carrier concentrations of the 2×10^{15} cm^{-2} case decrease at first and then increase in the temperature range above 850°C. With regard to the

4×10^{14} cm^{-2} case, the carrier concentrations show a similar trend to the 2×10^{15} cm^{-2} ones but eventually saturate when the annealing temperature exceeds 1000°C. For the B$^+$-implanted films with different dosage, the carrier concentrations increase, but the Hall mobilities decrease with increasing implantation dosage. As for the different annealing temperature, carrier concentrations and mobilities gradually increase and saturate above 1000°C for the three kinds of dosages.

The mobility is related to sheet resistance and carrier concentration. For a uniformly doped thin film, the sheet resistance (R_s) can be expressed as

$$R_s = 1 / (N_a q \mu_{eff} t),$$

where q is the electronic charge, N_a is the average carrier concentration, μ_{eff} is the effective carrier mobility, and t is the film thickness. The sheet resistance increases when the carrier concentration decrease exceeds the mobility increase and vice versa. This relationship also corresponds to the results shown in Fig. 4. The improvement in mobilities was examined by TEM observation. Figs. 5a, 5b, and 5c show the TEM observations of the films implanted by arsenic ions with the 2×10^{15} cm^{-2} dose and annealed at 700, 800, and 1000°C for 1 h, respectively. In these photographs, it is found that the annealed samples with larger grain size and minor intragranular defects show higher mobility. It is also worth noting that the samples annealed at 1000°C
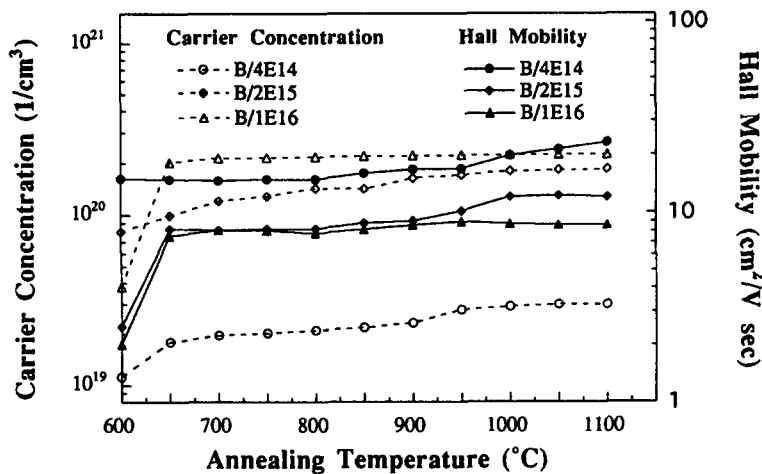

Fig. 4. Carrier concentrations and mobilities of the B$^+$-implanted samples treated with different annealing temperatures.

show equiaxial grain structures with fewer microdefects, which are obviously different from those films with dendritic grain structures annealed at lower temperatures. The structural differences of the specimens are attributed to different grain growth mechanisms under the different annealing temperatures [7]. Fig. 6 shows the microstructures of the films implanted by B^+ with the 2×10^{15} cm^{-2} dose and annealed at 1000°C for 30 min. The microstructures of the films annealed at lower temperature also have a similar structure but a slightly smaller grain size than that annealed at 1000°C. The higher carrier mobility for the higher temperature is also realized for larger grain size.
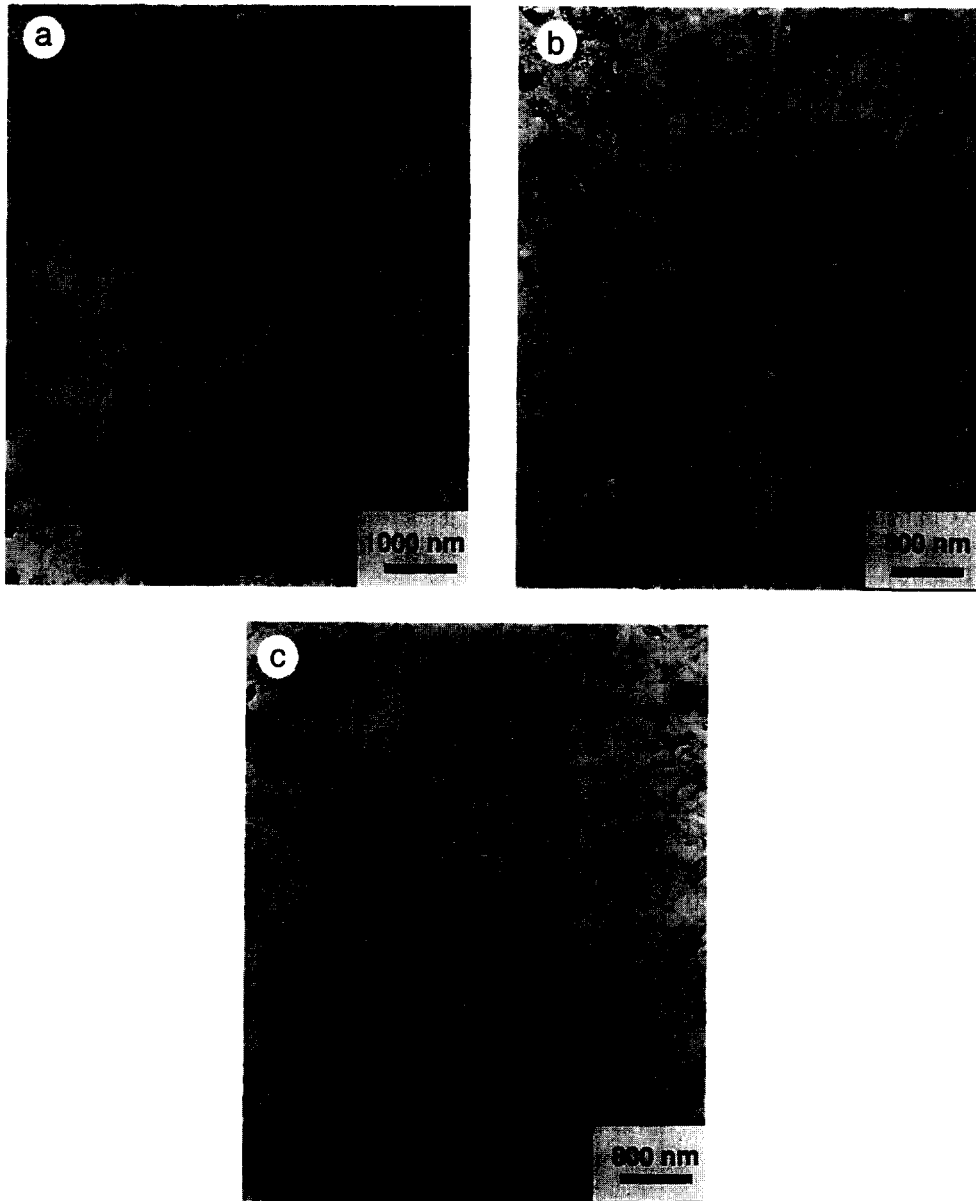

Fig. 5. TEM photographs of films implanted by As$^+$ with the 2×10^{15} cm^{-2} dose and annealed at (a) 700°C, (b) 800°C, and (c) 1000°C, respectively.
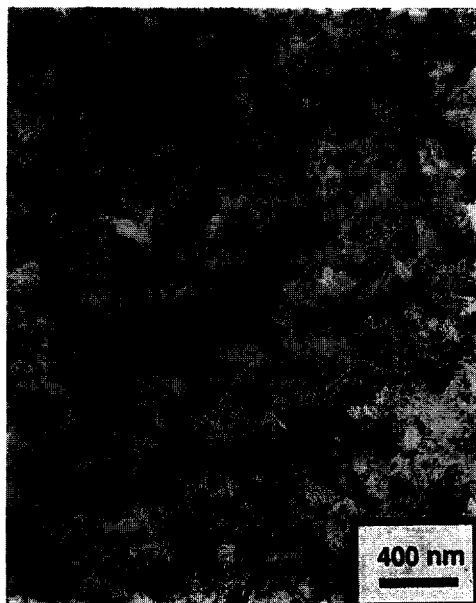
Fig. 6. TEM photographs of films implanted by B^+ with the 2×10^{15} cm^{-2} dose and annealed at 1000°C.

For the As-implanted samples, both dopant activation and dopant segregation occur simultaneously in the annealing process. The former increases the carrier concentration and is influenced by the solid solubility of the poly-Si grains at the annealing temperature. The latter causes the activated dopants to diffuse to the poly-Si/SiO$_2$ interface or the grain boundaries and results in decrease of the carrier concentration. The reverse annealing in the sheet resistances for the 2×10^{15} cm^{-2} specimens are attributed to the segregation of the activated dopants during annealing. It results in the decrease of the carrier concentration from 700 to 850°C. The reverse tendency of the carrier concentrations at higher annealing temperatures is ascribed to the increasing intragranular solid solubility and the decreasing intragranular dopant segregation at higher temperatures. For the heavily implanted samples (the 1×10^{16} cm^{-2} case), since the amount of the segregated dopants is much less than the total dopant concentration, the increase of the dopant activation with annealing temperature will be dominant, causing the monotonically decrease of the sheet resistance. With regard to the 4×10^{14} cm^{-2} implanted films, the

reverse annealing becomes even more marked, indicating that the extent of dopant segregation is greater for the lower implantation dosage.

According to the carrier trapping model [8], the carrier transport in poly-Si is influenced by potential barriers at the grain boundaries and the carrier traps in intragranular microdefects. For the low-temperature annealed samples, the microdefects in the grown grains cause the low electron mobility. With the release of microdefects due to higher annealing temperatures, the electron mobilities are thus promoted. Similarly, the higher electron mobilities for the 2×10^{15} cm^{-2} for the 4×10^{14} cm^{-2} specimens are also attributed to lower potential barriers due to the higher carrier concentrations. However, the impurity scattering in the heavily doped films leads to lower electron mobilities for the 1×10^{16} cm^{-2} implanted ones.

The electrical properties (sheet resistance, carrier concentration, and mobility) which are monotonic functions of the annealing temperature show that dopant activation of the B^+-implanted specimens is very different from annealed As$^+$-implanted samples. No reverse annealing phenomenon found implies that boron does not segregate at grain boundaries or trap in microdefects. As the annealing temperature increases up above 1000°C, the saturation of carrier concentration results from the limit of the solid solubility of the B^+-implanted α-Si films [1]. The excess boron in annealed samples form Si-B compounds or precipitate in the interior of grains and impurity scattering to influence the carrier transport. Such precipitation caused by heavily B^+ implantation would suppress grain growth and therefore decrease mobilities.

4. Conclusions

In summary, dosage dependence of the reverse annealing phenomenon for As$^+$-implanted α-Si films has been observed. This phenomenon becomes more marked with decreasing implantation dosage. Dopant segregation causes the reduction of carrier concentrations for moderate doping levels, whereas the solid solubility becomes dominant for the heavily implanted samples. As for the B^+-implanted α-Si films,

the impurity scattering becomes dominant for carrier transport. The dopants do not segregate at grain boundaries but may precipitate in the interior of grains when the dopant concentration exceeds its solid solubility.

Acknowledgements

References

[1] T. Kamins, Polycrystalline Silicon for Integrated Circuit Applications (Kluwer, Boston, 1988).

[2] T.H. Ning and R.D. Isaac, IEEE Trans. Electron Devices 32 (1980) 242.

[3] H. Ryssel, H. Iberl, M. Bleier, G. Prinke, K. Haberger and H. Kranz, Appl. Phys. 24 (1981) 197.

[4] E.G. Lee and H.B. Im, J. Electrochem. Soc. 138 (1991) 3465.

[5] R.A. Powell and R. Chow, J. Electrochem. Soc. 132 (1985) 194.

[6] M.H. Juang and H.C. Cheng, Appl. Phys. Lett. 60 (1992) 2092.

[7] A. Nakamura, F. Emoto, E. Fujii, A. Yamamoto and Y. Uemoto, J. Appl. Phys. 66 (1989) 4248.

[8] G. Baccarani and B. Ricco, J. Appl. Phys. 49 (1978) 5565.